Assessment of DFT functionals with NMR chemical shifts

Robert Laskowski and Peter Blaha
Institute of Materials Chemistry, Vienna University of Technology, Getreidemarkt 9/165-TC, A-1060 Vienna, Austria

Fabien Tran
Institute of Physical Chemistry, University of Zurich, Winterthurerstrasse 190, CH-8057 Zurich, Switzerland
(Received 26 February 2013; revised manuscript received 29 April 2013; published 23 May 2013)

Density-functional theory (DFT) calculations of the magnetic shielding for nuclear magnetic resonance (NMR) in solids provide an important contribution for understanding the experimentally observed chemical shifts. It is known that the calculated NMR shielding parameters for a particular nucleus in a series of compounds correlate well with the experimentally measured chemical shifts; however, the slope of a linear fit often differs from the ideal value of 1.0. Focusing on a series of ionic compounds (fluorides, oxides, bromides, and chlorides), we show that the error is caused by the generalized gradient approximation (GGA) to the exchange-correlation functional and it is related to the well-known band-gap problem. In order to devise an *ab initio* approach that would correctly reproduce the variation of the shifts within a series of compounds, we test various DFT based approaches. A simple GGA + U scheme with the orbital field acting on the cation d states does not work in a general way. Also, the popular hybrid functionals (including the screened versions), which contain some fixed amount of exact exchange, lead to a large overestimation of the necessary slope correction. Surprisingly, the best solution to this problem is offered by a semilocal potential designed by Becke and Johnson to reproduce the optimized exact exchange potential in free atoms.

DOI: 10.1103/PhysRevB.87.195130 PACS number(s): 71.45.Gm, 76.60.Cq, 71.15.−m

I. INTRODUCTION

Nuclear magnetic resonance (NMR) is a powerful and widely used experimental method that provides information about the atomic and electronic structure of materials.[1] It measures the response of a material to an external magnetic field by detecting the transition energies related to the reorientation of the nuclear magnetic moment. The external field induces an electronic current in the sample, which according to Biot-Savart's law produces an induced field that partially screens the external field. The NMR transition energies are proportional to the total magnetic field at the nucleus. The induced current and the corresponding shielding depend strongly on the electronic and atomic structures of the material. In order to interpret the experimental results, it is essential to understand this rather complicated and indirect relation. In the case of organic molecules and H or C nuclei a set of empirical rules are already established and routinely applied.[2] However, for other (heavier) nuclei, or larger molecules and in particular for solids, such rules are more difficult to build[3–8] and the interpretation of the experimental data is a more complicated task.[9,10] The interpretation procedure can be aided by *ab initio* calculations provided that the computed spectra can properly reproduce the experimental results.[11–13] So far mostly density-functional theory (DFT) in the generalized gradient approximation (GGA) has been applied to NMR calculations in solids. However, in many cases the *ab initio* approaches have some difficulties reaching the desired accuracy. The problems manifest mainly in the common observation that within a series of compounds the computed shielding parameters for a particular nucleus show systematic error when compared to the measured values.[12,14–19] For example, in the case of fluorides or oxides the shielding parameters computed within DFT using the standard Perdew-Burke-Ernzerhof (PBE)[20] exchange-correlation functional correlate well with the measured values, but the slope of the line representing the relation between the experimental and theoretical data is close to 0.8 instead of 1.0.[14,15] This intriguing and very systematic error has its origin in the deficiencies of the approximate density functional. For instance, it has been shown before that for the ^{17}O chemical shift the error in CaO is significantly larger than for many other oxides and that the problem arises due to Ca 3d orbitals being too close to the valence-band maximum,[12] which affects the Ca-3d O-2p hybridization.

In this paper we focus our discussion on the variation of the chemical shifts in series of fluorides, chlorides, bromides, and oxides. We intend to identify the origin of the systematic error manifested by the wrong "slope" in the correlation between theory and experiment and investigate possible solutions to this problem. In this perspective our analysis will provide useful hints not only to improve the calculations of the NMR shielding parameters in solids, but we suggest that such chemical shift calculations may also provide a sensitive test to assess the quality of a particular approximate DFT functional.

II. THEORETICAL APPROACH

Until now several methods of *ab initio* calculation of NMR chemical shifts for molecules[21,22] and solids have been described in the literature.[23–27] In the case of solids they usually operate within the standard DFT[28,29] framework.

The implementation used in this work is based on a linear-response approach[23,25,30] and the all-electron augmented plane-wave (APW) method.[31,32] The details are described in a previous publication.[33] Here we outline only the essential points necessary for further discussion.

The shielding tensor $\overleftrightarrow{\sigma}$ is defined as the proportionality constant between the induced magnetic field $\mathbf{B}_{\mathrm{ind}}$ measured at

the nucleus at site $\mathbf{R}$ and the external field $\mathbf{B}$:

$$\mathbf{B}_{\rm ind}(\mathbf{R}) = -\overleftrightarrow{\sigma}(\mathbf{R})\mathbf{B}. \quad (1)$$

Often, only the information about the isotropic shielding (IS) $\sigma(\mathbf{R}) = \mathrm{Tr}[\overleftrightarrow{\sigma}(\mathbf{R})]$ can be accessed by experiment. Moreover, the experimentally measured quantity is the chemical shift δ, which is the NMR shielding obtained with respect to some reference compound, $\delta(\mathbf{R}) = \sigma_{\rm ref} - \sigma(\mathbf{R})$.

The induced field $\mathbf{B}_{\rm ind}$ is obtained by integrating the induced current $\mathbf{j}_{\rm ind}(\mathbf{r})$ according to the Biot-Savart law:

$$\mathbf{B}_{\rm ind}(\mathbf{R}) = \frac{1}{c}\int d^3r\,\mathbf{j}_{\rm ind}(\mathbf{r}) \times \frac{\mathbf{R}-\mathbf{r}}{|\mathbf{r}-\mathbf{R}|^3}. \quad (2)$$

For nonmagnetic and insulating materials, only the orbital motions of electrons contribute to $\mathbf{j}_{\rm ind}(\mathbf{r})$. In such a case, the induced current is calculated in the framework of perturbation theory, where the first-order perturbation of the Hamiltonian in the symmetric gauge is given by

$$H^{(1)} = \frac{1}{2c}\mathbf{r}\times\mathbf{p}\cdot\mathbf{B}. \quad (3)$$

Within DFT the current density is evaluated as a sum of expectation values of the current operator running over the occupied Kohn-Sham (KS) states:

$$\mathbf{J}(\mathbf{r}') = -\frac{\mathbf{p}|\mathbf{r}'\rangle\langle\mathbf{r}'| + |\mathbf{r}'\rangle\langle\mathbf{r}'|\mathbf{p}}{2} - \frac{\mathbf{B}\times\mathbf{r}'}{2c}|\mathbf{r}'\rangle\langle\mathbf{r}'|. \quad (4)$$

The expression for the induced current involves only the first-order terms with respect to the external field $\mathbf{B}$:

$$\mathbf{j}_{\rm ind}(\mathbf{r}') = \sum_o \left[\left\langle\Psi_o^{(1)}\middle|\mathbf{J}^{(0)}(\mathbf{r}')\middle|\Psi_o^{(0)}\right\rangle + \left\langle\Psi_o^{(0)}\middle|\mathbf{J}^{(0)}(\mathbf{r}')\middle|\Psi_o^{(1)}\right\rangle + \left\langle\Psi_o^{(0)}\middle|\mathbf{J}^{(1)}(\mathbf{r}')\middle|\Psi_o^{(0)}\right\rangle\right], \quad (5)$$

where $\Psi_o^{(0)}$ is an unperturbed Kohn-Sham (KS) occupied orbital, $\mathbf{J}^0(\mathbf{r}')$ is the paramagnetic part of the current operator [the first term in Eq. (4)], and $\mathbf{J}^1(\mathbf{r}')$ is the diamagnetic component of the current operator [the second term in Eq. (4)]. $\Psi_o^{(1)}$ is the first-order perturbation of $\Psi_o^{(0)}$ with respect to $H^{(1)}$ expressed using the usual formula:

$$\left|\Psi_o^{(1)}\right\rangle = \sum_e \left|\Psi_e^{(0)}\right\rangle \frac{\left\langle\Psi_e^{(0)}\middle|H^{(1)}\middle|\Psi_o^{(0)}\right\rangle}{\epsilon_o - \epsilon_e}, \quad (6)$$

with the sum running over all empty (unoccupied) KS orbitals. Here we should stress that Eq. (5) is used as the reference formula in order to discuss the physics, while the actual formulas specific to our augmented plane-wave plus local-orbital (APW + lo) implementation are given in Ref. 33. We stress that, contrary to the reference formula Eq. (5), our actual implementation is gauge invariant and the results do not depend on the choice of the unit-cell origin.

The calculations presented in this work have been performed using the WIEN2K code[32] and are based on the APW + lo method and DFT. Within this method the unperturbed wave functions as well as their first-order perturbations are expressed using plane waves in the interstitial region and an atomiclike representation inside the atomic spheres S_α:

$$\Psi_{n,\mathbf{k}}(\mathbf{r}) = \begin{cases} \frac{1}{\sqrt{\Omega}}\sum_{\mathbf{G}} C_G^{n,\mathbf{k}} e^{i(\mathbf{G}+\mathbf{k})\cdot\mathbf{r}}, & \mathbf{r}\in I \\ \sum_{lm} W_{lm}^{n,\alpha,\mathbf{k}}(r)Y_{lm}(\hat{r}), & \mathbf{r}\in S_\alpha. \end{cases} \quad (7)$$

The APW basis set is naturally optimized for occupied states by expanding the numerical radial basis functions at predefined linearization energies,[31] which are chosen to match the energies of the corresponding occupied bands. This approach yields basically the exact radial wave functions for all occupied states. However, in NMR calculations we expand the perturbation of the wave functions due to the magnetic field using high-lying (unoccupied) eigenstates [see the linear perturbation formula in Eq. (6)]. Therefore, NMR shielding calculations require an extended basis set inside the atomic spheres. This is achieved by supplying additional local orbitals as described in Ref. 33. This extension is done for all orbital quantum numbers up to $l+1$, where l is the maximal occupied orbital quantum number of the valence states of the specific atom. For other computational parameters, the standard values lead to well-converged results. The plane-wave cutoff was set according to $R_{\rm min}K_{\rm max} = 8$ ($R_{\rm min}$ is the smallest sphere radii in the system, and $K_{\rm max}$ is the plane-wave momentum cutoff). The Brillouin zone was sampled with a mesh step approximately equal to 0.02 Å^{-1}. All calculations have been performed using scalar relativistic approximation.[34] We also have tested the effect of spin-orbit coupling, but even in the heavier cases like CsBr or CsCl it is on the level of 1 ppm only.

III. RESULTS

The comparison of the measured NMR shifts with the NMR shielding calculated with the PBE[20] exchange-correlation functional for ^{19}F and ^{17}O nuclei in metal fluorides and oxides is presented in Fig. 1 (black squares). For both nuclei the measured and calculated parameters correlate quite well (the standard deviation of the slope as well as the root-mean-square deviation (RMSD) value are indicated in the figures); however, the slope of a linear fit is considerably different from the correct value of -1.0. We have analyzed the origin of the observed trend within the fluorides series previously,[37] but repeat here the main conclusions, since the understanding of the relation between the electronic structure and the NMR shielding is necessary to identify the source of errors in the computed shielding parameters.

The contributions to the ^{19}F chemical shifts originating from the F-1s and F-2s states are large but constant for all compounds in the series.[37] The variation of the shielding thus comes solely from bands with predominantly metal-p and F-p characters (all cations except Li and Be have a "semicore" p band several eV below the F-2p valence band). These states couple due to the external magnetic field [Eq. (6)] to unoccupied states with metal-d and F-d character. Again, the contribution related to the direct coupling of valence F-p and F-d states is fairly constant for all fluorides, and it is the (indirect) coupling to the metal-d states which determines the variation of the chemical shift within the series of compounds. This indicates the importance of hybridization between F-p and metal-p states because it allows us to transfer the effect to the F atom. Obviously, the amount of metal-p character in the F-p bands and F-p character in the metal-p bands depends on the energy separation between those bands. The metal-p bands are always below the F-p bands, and thus the orbital mixing is bonding in character in the metal-p bands (the same phase) and antibonding in the F-p bands (the opposite phase).

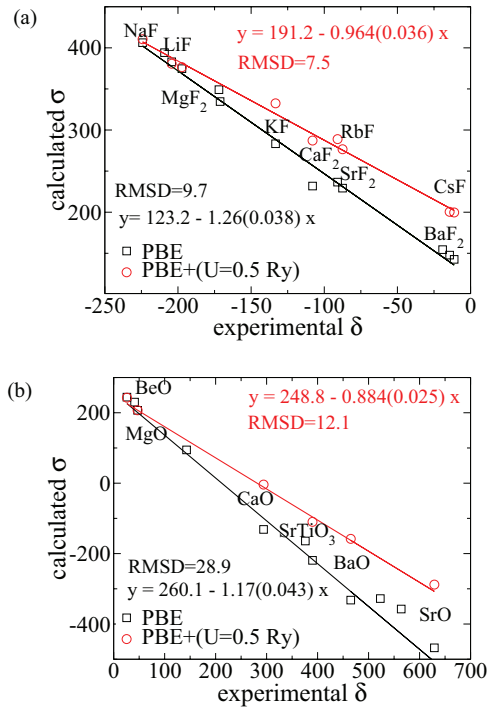

FIG. 1. (Color online) The correlation between measured isotropic chemical shifts and calculated isotropic NMR shielding (in ppm) for (a) ^{19}F in metal fluorides and (b) ^{17}O in metal oxides. The results calculated with PBE are compared to PBE + U (U_{eff} = 0.5Ry). The experimental values for ^{19}F are taken from Ref. 15 and for ^{17}O are taken from Refs. 14,35 and 36.

As a result the contributions to the shift coming from these two sets of bands have opposite signs. In summary, the major factors determining the behavior of the ^{19}F shielding within a series of compounds are the energy separation between the F-p and metal-p bands and the position of the empty metal-d states. The energy separation between F-p and metal-p states is decreasing for heavier metal atoms and thus leading to larger hybridization. The empty metal-d states come down in energy for heavier elements, leading to a larger coupling strength. The analysis presented for the fluoride series[37] can also be performed for oxides, leading to very similar conclusions.

We see in Fig. 1 that the slope of a linear fit is equal to (minus) 1.26 and 1.17 for the ^{19}F and ^{17}O series, respectively. Thus, the error reaches 25% when comparing ^{19}F shifts in compounds with light and heavy elements. Since the absolute value of the NMR shielding is not accessible experimentally, we limit the further discussion to those details which are responsible for the variation of the shielding between different compounds within a series. The analysis summarized above indicates that there are two possible sources of errors leading to the wrong slope of the regression in Fig. 1: first an error in the strength of the hybridization between metal-p and O or F-p states, and second an incorrect coupling between the occupied metal-p and empty metal-d states.

The first possibility cannot be the dominant effect, since one would need a rather large change in the metal-p and F-p hybridization to affect the NMR shielding sufficiently. This becomes quite clear when we directly investigate the effect by

TABLE I. The dependence of the F isotropic shielding (σ_{iso}) (in ppm), the energy separation $\Delta_{\text{Cs-}p,\text{F-}p}$ (in Ry), and the partial charges (e^-) of F-p character in the Cs-p bands (Q_{F} in Cs) and Cs-p in F-p bands (Q_{Cs} in F) on the value of U (in Ry) acting on the Cs-p states in GGA + U calculations for Cs-F. The partial charges Q_{F} and Q_{Cs} are the results of integration of charge densities for particular sets of bands within F and Cs atomic spheres.

U_{eff} (Ry)	$\Delta_{\text{Cs-}p,\text{F-}p}$	Q_{F} in Cs-p	Q_{Cs} in F-p	σ_{iso}
0.0	0.360	0.1122	0.2228	142.6
0.1	0.374	0.1026	0.2096	148.3
0.2	0.386	0.0938	0.1972	155.0
0.3	0.400	0.0856	0.1854	161.7
0.4	0.414	0.0780	0.1744	168.4

manipulating the position of the metal-p band relative to the F-p band. It can be done using an orbital-dependent potential acting only on the metal-p states, as is possible with the GGA + U method.[38] In a simplified form the orbital potential can be expressed by

$$V^{\text{FLL}} = U_{\text{eff}} \left(\tfrac{1}{2} - \hat{n}_\ell\right), \tag{8}$$

where $\hat{n}_\ell$ is the occupancy of the orbitals with angular momentum ℓ. The metal-p bands are of course fully occupied; therefore, any positive U_{eff} generates an attractive potential and shifts the metal-p states down with an amount proportional to U_{eff}. This shift changes the hybridization of the F-p and metal-p states. Table I presents the effect using CsF as an example. We can see that with $U_{\text{eff}} = 0.4$Ry a change of more than 25% of the F partial charges (Q_{F}) in the Cs-p band and the Cs partial- harge (Q_{Cs}) in the F-p bands can be achieved, but this results only in a 27-ppm change of σ_{iso}, while we would need a twice as large effect to get the correct slope. For comparison, the difference generated by using PBE and Becke-Johnson (BJ) (see below) exchange-correlation functionals is less than 4% of the partial charges.

On the other hand, we know that GGA-DFT calculations underestimate considerably band gaps of semiconductors and insulators, and this could be the major source of error. This means that the unoccupied metal-d states are too low in energy, leading to an overestimated coupling between metal-p and metal-d states because the denominator in Eq. (6) is too small. Using a similar GGA + U approach as described above, but now acting on the empty metal-d states, we can manipulate the position of the metal-d character in the conduction band. Assuming the metal-d states are empty (the method can be applied only to atoms that do not have an occupied d shell), any positive value of U_{eff} will generate a repulsive potential for the d states and increase the energies of those orbitals. As a consequence, we should observe a weakening of the coupling between metal-p and metal-d bands, which decreases the valence contribution to the shielding and increases the total NMR shielding. The effect of course depends on the initial position of the metal-d states and the hybridization between metal and nonmetal p states in a compound. In the case of Li, where there are no d states present in the vicinity of the band gap, we do not observe any change. However, for heavy elements like Cs, where the d states are closer to the valence-band maximum and the Cs-p band is relatively high

in the valence region of the spectra, the effect is large. This is essentially what is presented in Fig. 1 (red circles and lines). Interestingly, the NMR shifts produced by PBE + U still align nicely on a straight line for both cases. We have chosen U_{eff} equal to 0.5Ry for both fluorides and oxides, so that the slope of the linear least-square fit is now close to 1.0 for the fluorides. However, the choice of U_{eff} grossly overestimates the effect on oxides and reduces the corresponding slope to below 0.9. Of course it is possible to find specific values of U (different for fluorides and oxides) that lead to the correct slope in both cases, but it would be difficult to justify the approach in some cases, which makes it not usable for any predictions. For instance, U_{eff} for Ba-d states should be different in BaF_2 and BaO. At this point it is clear that we need a method which can describe both the hybridization between cationic and anionic states and the position of empty metal-d bands properly. By choosing the proper U value, we can reproduce the experimental shielding, but PBE + U is not able to capture the difference between the screening properties of oxides and fluorides and at the same time correctly position the d character in the conduction band with a single value for U_{eff}.

In quantum chemistry the chemical shifts of molecules are calculated quite often using a hybrid functional approach, where a certain fraction of Hartree-Fock exchange is added to DFT. We explore here the effect of hybrid functionals on the chemical shifts for solids. We use the Yukawa screened version of PBE0 implemented in the WIEN2K code,[39,40] where a fraction of $\alpha = 0.25$ of the total exchange is described by Hartree-Fock exchange while the remaining fraction of exchange as well as correlation is covered by the PBE functional. The implementation is based on a formalism by Massidda, Posternak, and

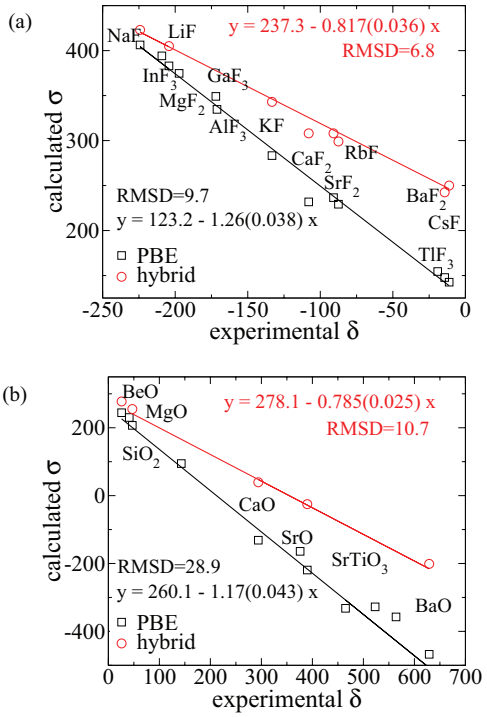

FIG. 2. (Color online) The correlation between measured isotropic chemical shifts and calculated NMR shielding (in ppm) for (a) ^{19}F in metal fluorides and (b) ^{19}O in metal oxides series. PBE results are compared to calculations using the YS-PBE0 hybrid functional. The experimental values for ^{19}F are taken from Ref. 15 and for ^{16}O are taken from Refs. 14,35 and 36.

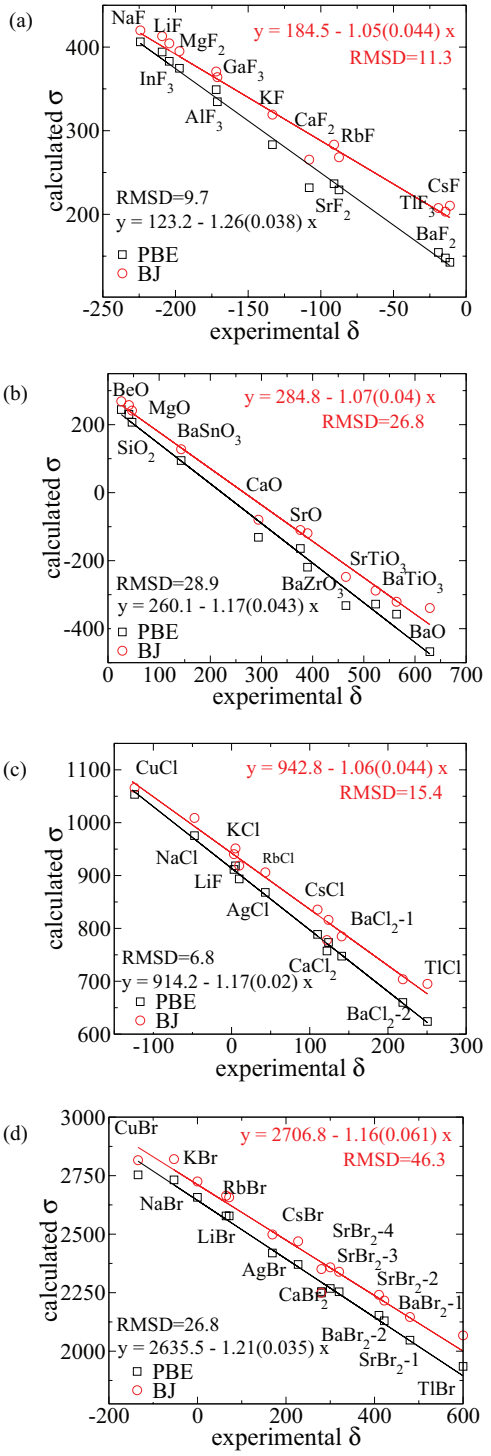

FIG. 3. (Color online) The correlation between the measured chemical shifts and calculated NMR shielding (in ppm) for (a) ^{19}F in metal fluorides, (b) ^{16}O in metal oxides, (c) $^{79/81}$Cl in metal chlorides, and (d) $^{35/37}$Br in metal bromides. The calculations have been performed with PBE and Becke-Johnson exchange-correlation potentials. The experimental values for ^{19}F are taken from Ref. 15; for ^{16}O are taken from Refs. 14,35 and 36; and for $^{35/37}$Br and $^{79/81}$Cl are taken from Refs. 44 and 45.

TABLE II. The isotropic shielding σ_{iso}^{LAPW} computed with PBE and BJ-LDA exchange-correlation potentials for ^{19}F in fluorides, ^{17}O in oxides, $^{35-37}$Cl in chlorides, and $^{79-81}$Br in bromides, where LAPW stands for linearized augmented plane wave. We compare our results with available shieldings computed with GIPAW, as well as to measured NMR chemical shifts. The experimental shifts δ_{iso}^{expt} are given with reference to $CFCl_3$ for ^{19}F, H_2O for ^{17}O, KBr for $^{79-81}$Br, and 1 M NaCl(aq) for $^{35-37}$Cl. The theoretical shifts δ_{iso}^{LAPW} are given with a reference taken from the linear fit equations included in Fig. 3. All values are in ppm. For all calculations experimental lattice parameters are taken from the inorganic crystal structure database.[46]

	Space group	$\sigma_{iso}^{LAPW,PBE}$	$\sigma_{iso}^{LAPW,BJ}$	$\sigma_{iso}^{GIPAW,PBE}$	$\delta_{iso}^{LAPW,PBE}$	$\delta_{iso}^{LAPW,BJ}$	δ_{iso}^{expt}
Fluorides							
LiF	*Fm*-3*m*	383.0	404.4	369.3[15]	−259.8	−219.9	−204.3[15]
NaF	*Fm*-3*m*	406.3	419.9	395.8[15]	−283.1	−235.4	−224.2[15]
KF	*Fm*-3*m*	283.3	319.2	268.1[15]	−160.1	−134.7	−133.3[15]
RbF	*Fm*-3*m*	236.6	283.3	221.3[15]	−113.4	−98.8	−90.9[15]
CsF	*Fm*-3*m*	142.6	210.3	136.3[15]	−19.4	−25.8	−11.2[15]
MgF_2	*P*42/*mnm*	374.7	395.1	362.7[15]	−251.5	−210.6	−197.3[15]
CaF2	*Fm*-3*m*	231.8	265.4	220.0[15]	−108.6	−80.9	−108.0[15]
SrF_2	*Fm*-3*m*	229.3	268.3	215.3[15]	−106.1	−83.8	−87.5[15]
BaF_2	*Fm*-3*m*	147.8	203.2	151.9[15]	−24.6	−18.7	−14.3[15]
α-AlF3	*R*-3*c*	349.1	370.8	-	−225.9	−186.3	−172.0[47]
GaF_3	*R*-3*c*	334.6	364.1	-	−211.4	−179.6	−171.2[3]
InF3	*R*-3*c*	394.2	413.0	-	−271.0	−228.5	−209.2[3]
TlF	*Pbcm*	154.5	207.5	-	−31.3	−23.0	−19.1[48]
Oxides							
BeO	*P*63*mc*	244.3	268.8	232.2[14]	15.8	16.0	26[35]
MgO	*Fm*-3*m*	207.0	241.3	198.0[14]	53.1	43.5	47[35]
SrO	*Fm*-3*m*	−219.2	−119.3	−205.2[14]	479.3	404.1	390[35]
BaO	*Fm*-3*m*	−467.6	−339.3	−444.3[14]	727.7	624.1	629[35]
$SrTiO_3$	*Pm*-3*m*	−332.1	−247.7	−287.3[14]	592.2	532.5	465[36]
CaO	*Fm*-3*m*	−131.4	−79.7	−156.6[12]	391.5	364.5	294[12]
SiO_2	*P*3221	230.2	257.6	313.3[49]	29.9	27.2	41[49]
$BaZrO_3$	*Pm*-3*m*	−164.2	−109.9	−172.8[14]	424.3	394.7	376[36]
$BaSnO_3$	*Pm*-3*m*	94.5	127.8	98.0[14]	165.6	157.0	143
$BaTiO_3$	*P*4*mm*	−357.4	−320.9	−357.9[14]	617.5	605.7	564[14]
		−327.7	−288.0	−347.4[14]	587.8	572.8	523[14]
Chlorides							
LiCl	*Fm*-3*m*	918.4	951.3		−4.2	−8.5	5.0[44,50]
NaCl	*Fm*-3*m*	975.5	1009.0		−61.3	−66.2	−47.4[44,50]
KCl	*Fm*-3*m*	911.5	940.5		2.7	2.3	3.1[44,50]
AgCl	*Fm*-3*m*	893.6	918.8		20.6	24.0	9.8[44,51]
CsCl	*Pm*-3*m*	788.7	835.6		125.5	107.2	110[44,50]
RbCl	*Fm*-3*m*	868.1	906.1		46.1	36.7	43.2[44,50]
CuCl	*F*-43*m*	1053.5	1066.0		−139.3	−123.2	−124[44,51]
TlCl	*Pm*-3*m*	623.9	695.1		290.3	247.7	250.5[44]
$CaCl_2$	*Pnnm*	757.3	777.9		156.9	164.9	122[44,52]
$BaCl_2$	*Pnma*	773.5	816.1		140.7	126.7	124[44,53]
		659.9	703.8		254.3	239.0	219[44,53]
$SrCl_2$	*Fm*-3*m*	747.5	784.9		166.7	157.9	140.8[44,50]
Bromides							
KBr	*Fm*-3*m*	2657.1	2725.2		−21.6	−18.4	0[44,45]
LiBr	*Fm*-3*m*	2578.0	2664.3		57.5	42.5	64.7[44,45]
NaBr	*Fm*-3*m*	2732.0	2820.7		−96.5	−113.9	−52.9[44,45]
Rbr	*Fm*-3*m*	2578.1	2657.5		57.4	49.3	71.7[44,45]
CsBr	*Pm*-3*m*	2370.6	2469.4		264.9	237.4	227.4[44,45]
AgBr	*Fm*-3*m*	2419.6	2498.8		215.9	208.0	169.3[44,45]
$CaBr_2$	*Pnnm*	2248.7	2249.9	2266.7[a][18]	386.8	456.9	280[18]
$SrBr_2$	*P*4/*nz*	2130.0	2216.3	2169.8[a][18]	505.5	490.5	422[18]

TABLE II. (*Continued*).

	Space group	$\sigma_{iso}^{LAPW,PBE}$	$\sigma_{iso}^{LAPW,BJ}$	$\sigma_{iso}^{GIPAW,PBE}$	$\delta_{iso}^{LAPW,PBE}$	$\delta_{iso}^{LAPW,BJ}$	δ_{iso}^{expt}
		2153.5	2240.7	2194.4[a][18]	482.0	466.1	410[18]
		2254.2	2339.4	2290.7[a][18]	381.3	367.4	320[18]
		2268.7	2358.4	2304.7[a][18]	366.8	348.4	300[18]
$BaCl_2$		2254.8	2351.0	2323.8[a][18]	380.7	355.8	280[18]
		2047.1	2146.1	2124.3[a][18]	588.4	560.7	480[18]
TlBr	*Pm-3m*	1935.8	2067.6		699.7	639.2	600[44,54]
CuBr	*F-43m*	2753.4	2816.1		−117.9	−109.3	−134.1[44,45]

[a]The cited shielding has been converted to absolute shifts using our value for KBr.

Baldereschi[41] originally developed for the unscreened Hartree-Fock exchange. The comparison between the NMR shielding computed with PBE and YS-PBE0 is presented in Fig. 2. Hybrid functionals usually increase the band gaps between valence and conduction bands in semiconductors as compared to the PBE calculations. Therefore, it is not surprising that the NMR shielding parameters are larger for YS-PBE0 than for PBE. The explanation of this effect follows the same arguments as presented above for GGA + U calculations. Unfortunately, the changes are much too strong, leading to linear fits with much too small slopes. We can see in Fig. 2 that the slope is around 0.8 for both fluorides and oxides, which at least indicates that the hybrid method is potentially more flexible than the simple PBE + U approach. Of course it would be possible to find an optimal value of the exact exchange mixing parameter α (around 0.1), which would lead to correct slopes for both oxides and fluorides at the same time. But such a value is significantly smaller than what is currently considered as standard in common hybrid functionals, and one would have to test its transferability to other materials and nuclei. Moreover, the method is computationally much more demanding compared to DFT with local or semilocal functionals, which inhibits its practical applications for large systems.

Another scheme which in principle could improve the description is the optimized effective potential (OEP) method for exact exchange. This should produce the exact Kohn-Sham exchange potential (the correlation part is still unknown), but the calculation of such OEP potential is quite cumbersome, expensive, and at least for all-electron methods numerically unstable.[42] Becke-Johnson[43] (BJ) derived a semilocal exchange potential, which reproduces the OEP potential in atoms very accurately. We have used the BJ exchange potential together with local-density approximation (LDA) correlation for the NMR shielding calculations, and the results are presented in Fig. 3. The calculated and experimental values show a nice linear correlation with a slope very close to 1.0 for the series of fluorides, oxides, and also chlorides. It should be noted that the BJ potential provides a parameter-free approximation to DFT, which seems to work equally well for these three very different series of compounds at the computational cost of a standard PBE calculation. In addition in Fig. 3 we also include results for metal bromides, where some level of improvement over PBE can be noticed, but it is much smaller than for the other series. At the moment it is difficult to speculate about the origin of the smaller improvement for the Br series. It could be that correlation has a more important role for these materials, which have a much smaller band gap than comparable chlorides or fluorides. The numerical results computed with PBE and BJ potentials for all compounds included in Fig. 3 are presented in Table II and compared to available theoretical gauge including projector augmented waves (GIPAW) calculations and experimental data. Overall, there is a very good agreement between the present PBE calculations and the GIPAW, results except for $SrTiO_3$ and SiO_2.

The sensitivity of the magnetic shielding on the electronic structure can be most easily demonstrated by comparing the density of states computed for CsF using different DFT approaches (Fig. 4). The Cs-p band around −5 eV is shifted slightly upward by BJ and YS-PBE0 methods as compared to PBE, but this has only a minor effect on σ (actually, it makes the slope even bigger). However, the upward shift of the Cs-d character in the conduction bands relative to PBE as evident for all functionals leads to a rather large change in the shielding (up to nearly 50 ppm, which is over 30% of the total shift). If this energy shift is so big that the computed band gap comes close to experiment, as in YS-PBE0, the correction to σ is grossly overestimated. A similar problem appears for the modified-BJ potential[55] (TB-mBJ), which yields energy band gaps in very good agreement with experiment or GW calculations and is even far superior to hybrid functionals for wide band-gap insulators. However, if

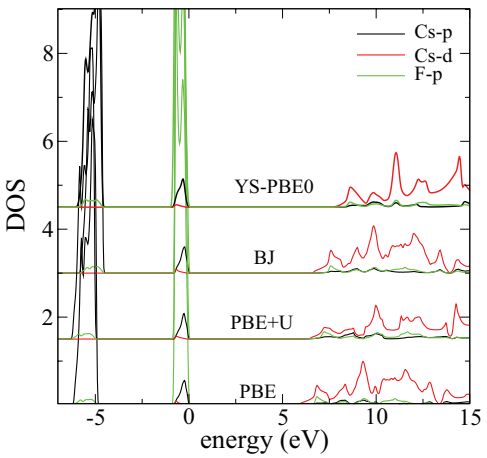

FIG. 4. (Color online) Partial density of states for CsF using different DFT exchange-correlation functionals. The plots are aligned to the valence-band maximum.

we apply the TB-mBJ potential for the magnetic shielding in fluorides we obtain a slope (0.73) which is even lower than that of YS-PBE0. We thus conclude that methods which reproduce the experimental gap more accurately (calculated from the eigenvalue differences only and without considering any exchange-correlation discontinuity) may not produce a good ground-state potential and related properties (other than the band gap) may not be accurate.

IV. CONCLUSIONS

NMR shielding parameters are very sensitive to the details of the electronic structure. The results for four different series of oxide and halide compounds indicate systematic errors in the computed NMR shielding parameters, which manifest themselves in a slope different from one when comparing experimental and theoretical shifts.

The hybridization between anion and cation electronic states in the occupied bands is of course very important, but small changes due to a modification of the relative energy position of the corresponding bands do not affect the computed NMR shielding too much. On the other hand, the position of the metal-*d* character in the unoccupied part of the band structure is very important and has a large influence on the magnetic shielding. We have tested several approaches that can potentially improve the DFT-PBE results. The semiempirical GGA + U approach can reproduce the experimental shifts properly; however, it requires a separate adjustment of the value of U for each compound series independently and is thus not a true *ab initio* method. The hybrid DFT methods with a standard mixing factor of 25% Hartree-Fock (PBE0) seem to overcorrect the electronic structure of the tested systems. In this case, the slope of the linear least-squares fit between experiment and theory is well below the ideal value 1.0, whereas for PBE it is larger than 1.0. Decreasing the mixing factor to roughly half of the PBE0 value would lead to more correct results. However, the hybrid scheme is computationally rather expensive, and essentially the mixing factor α is empirical; therefore, it is not very attractive for practical applications either. We found that at least for these exchange-dominated insulators a relatively simple and computationally inexpensive method leading to a fairly correct relation between experiment and theory is offered by the Becke and Johnson exchange potential, which is an approximation to OEP exact exchange.

Our analysis shows that the problems with theoretical calculation of NMR shielding parameters are related in fact to the DFT band-gap problem, but it is important to note that methods in which the eigenvalue difference of the valence-band maximum and conduction-band minimum reproduces the experimental gap are grossly overestimating the corrections of the magnetic shielding as compared to PBE results and are eventually even worse than PBE. Thus, a comparison of theoretical and experimental magnetic shielding (maybe together with a comparison of computed electric-field gradients and experimental quadrupole splittings)[56] may provide an interesting and alternative test of DFT functionals as compared to more common total-energy or band-gap calculations.

ACKNOWLEDGMENTS

We would like to acknowledge support by the Austrian Science Foundation (FWF) in Project No. SFB-F41 (ViCoM).

[1] *Encyclopedia of NMR*, edited by D. M. Grant and R. K. Harris (Wiley, New York, 1996).
[2] M. Schindler, J. Am. Chem. Soc. **109**, 1020 (1987).
[3] B. Bureau, G. Silly, J. Y. Buzaré, and J. Emery, Chem. Phys. **249**, 89 (1999).
[4] M. Body, G. Silly, C. Legein, and J.-Y. Buzaré, Inorg. Chem. **43**, 2474 (2004).
[5] M. Body, G. Silly, C. Legein, J.-Y. Buzaré, F. Calvayrac, and P. Blaha, J. Solid State Chem. **178**, 3655 (2005).
[6] C. Martineau, M. Body, C. Legein, G. Silly, J.-Y. Buzaré, and F. Fayon, Inorg. Chem. **45**, 10215 (2006).
[7] C. Legein, F. Fayon, C. Martineau, M. Body, J.-Y. Buzaré, D. Massiot, E. Durand, A. Tressaud, A. Demourgues, O. Péron, and B. Boulard, Inorg. Chem. **45**, 10636 (2006).
[8] A. Zheng, S.-B. Liu, and F. Deng, J. Phys. Chem. C **113**, 15018 (2009).
[9] P. d'Antuono, E. Botek, B. Champagne, J. Wieme, M.-F. Reyniers, G. B. Marin, P. J. Adriaensens, and J. M. Gelan, J. Phys. Chem. B **112**, 14804 (2008).
[10] C. Martineau, C. Legein, J.-Y. Buzaré, and F. Fayon, Phys. Chem. Chem. Phys. **11**, 950 (2009).
[11] A. J. Robbins, W. T. K. Ng, D. Jochym, T. W. Keal, S. J. Clark, D. J. Tozer, and P. Hodgkinson, Phys. Chem. Chem. Phys. **9**, 2389 (2007).
[12] M. Profeta, M. Benoit, F. Mauri, and C. J. Pickard, J. Am. Chem. Soc. **126**, 12628 (2004).
[13] T. Gregor, F. Mauri, and R. Car, J. Chem. Phys. **111**, 1815 (1999).
[14] D. S. Middlemiss, F. Blanc, C. J. Pickard, and C. P. Grey, J. Magn. Reson. **204**, 1 (2010).
[15] A. Sadoc, M. Body, C. Legein, M. Biswal, F. Fayon, X. Rocquefelte, and F. Boucher, Phys. Chem. Chem. Phys. **13**, 18539 (2011).
[16] C. M. Widdifield and D. L. Bryce, J. Phys. Chem. A **114**, 10810 (2010).
[17] M. Kibalchenko, J. R. Yates, C. Massobrio, and A. Pasquarello, Phys. Rev. B **82**, 020202(R) (2010).
[18] C. M. Widdifield and D. L. Bryce, J. Phys. Chem. A **114**, 2102 (2010).
[19] C. Bonhomme, C. Gervais, N. Folliet, F. Pourpoint, C. Coelho Diogo, J. Lao, E. Jallot, J. Lacroix, J.-M. Nedelec, D. Iuga, J. V. Hanna, M. E. Smith, Y. Xiang, J. Du, and D. Laurencin, J. Am. Chem. Soc. **134**, 12611 (2012).
[20] J. P. Perdew, K. Burke, and M. Ernzerhof, Phys. Rev. Lett. **77**, 3865 (1996).
[21] T. Helgaker, M. Jaszunski, and K. Ruud, Chem. Rev. **99**, 293 (1999).
[22] *Calculation of NMR and EPR Parameters. Theory and Applications*, edited by M. Kaupp, M. Buhl, and V. G. Malkin (Wiley, New York, 2004).

[23]F. Mauri, B. G. Pfrommer, and S. G. Louie, Phys. Rev. Lett. **77**, 5300 (1996).
[24]D. Sebastiani and M. Parrinello, J. Phys. Chem. A **105**, 1951 (2001).
[25]C. J. Pickard and F. Mauri, Phys. Rev. B **63**, 245101 (2001).
[26]T. Thonhauser, D. Ceresoli, A. A. Mostofi, N. Marzari, R. Resta, and D. Vanderbilt, J. Chem. Phys. **131**, 101101 (2009).
[27]D. Skachkov, M. Krykunov, and T. Ziegler, Can. J. Chem. **89**, 1150 (2011).
[28]P. Hohenberg and W. Kohn, Phys. Rev. **136**, B864 (1964).
[29]W. Kohn and L. J. Sham, Phys. Rev. **140**, A1133 (1965).
[30]J. R. Yates, C. J. Pickard, and F. Mauri, Phys. Rev. B **76**, 024401 (2007).
[31]D. J. Singh and L. Nordström, *Planewaves, Pseudopotentials and the LAPW Method*, 2nd ed. (Springer, New York, 2006).
[32]P. Blaha, K. Schwarz, G. K. H. Madsen, D. Kvasnicka, and J. Luitz, *WIEN2k, An Augmented Plane Wave Plus Local Orbitals Program for Calculating Crystal Properties* (Vienna University of Technology, Vienna, 2001).
[33]R. Laskowski and P. Blaha, Phys. Rev. B **85**, 035132 (2012).
[34]D. D. Koelling and B. N. Harmon, J. Phys. C **10**, 3107 (1977).
[35]G. L. Turner, S. E. Chung, and E. Oldfield, J. Magn. Reson. **64**, 316 (1985).
[36]T. J. Bastow, P. J. Dirken, M. E. Smith, and H. J. Whitfield, J. Phys. Chem. **100**, 18539 (1996).
[37]R. Laskowski and P. Blaha, Phys. Rev. B **85**, 245117 (2012).
[38]V. I. Anisimov, I. V. Solovyev, M. A. Korotin, M. T. Czyżyk, and G. A. Sawatzky, Phys. Rev. B **48**, 16929 (1993).
[39]F. Tran and P. Blaha, Phys. Rev. B **83**, 235118 (2011).
[40]F. Tran, D. Koller, and P. Blaha, Phys. Rev. B **86**, 134406 (2012).
[41]S. Massidda, M. Posternak, and A. Baldereschi, Phys. Rev. B **48**, 5058 (1993).
[42]M. Betzinger, C. Friedrich, A. Görling, and S. Blügel, Phys. Rev. B **85**, 245124 (2012).
[43]A. D. Becke and E. R. Johnson, J. Chem. Phys. **124**, 221101 (2006).
[44]C. M. Widdifield, R. P. Chapman, and D. L. Bryce, Annual Reports on NMR Spectroscopy **66**, 195 (2009).
[45]S. Hayashi and K. Hayamizu, Bull. Chem. Soc. Jpn. **63**, 913 (1990).
[46]http://icsd.fiz-karlsruhe.de/icsd/.
[47]P. J. Chupas, M. F. Ciraolo, J. C. Hanson, and C. P. Grey, J. Am. Chem. Soc. **123**, 1694 (2001).
[48]S. P. Gabuda, S. G. Kozlova, and R. L. Davidovich, Chem. Phys. Lett. **263**, 253 (1996).
[49]M. Profeta, F. Mauri, and C. J. Pickard, J. Am. Chem. Soc. **125**, 541 (2003).
[50]F. Lefebvre, J. Chim. Phys. Phys.-Chim. Biol. **89**, 1767 (1992).
[51]S. Hayashi and K. Hayamizu, J. Phys. Chem. Solids **53**, 239 (1992).
[52]T. O. Sandland, L.-S. Du, J. F. Stebbins, and J. D. Webster, Geochim. Cosmochim. Acta **68**, 5059 (2004).
[53]J. F. Stebbins and L.-S. Du, Am. Mineral. **87**, 359 (2002).
[54]T. Kanda, J. Phys. Soc. Jpn. **10**, 85 (1955).
[55]F. Tran and P. Blaha, Phys. Rev. Lett. **102**, 226401 (2009).
[56]P. Dufek, P. Blaha, and K. Schwarz, Phys. Rev. Lett. **75**, 3545 (1995).